

## IR Spectroscopy and Theory of $\text{Cu}^+(\text{H}_2\text{O})\text{Ar}_2$ and $\text{Cu}^+(\text{D}_2\text{O})\text{Ar}_2$ in the O–H (O–D) Stretching Region: Fundamentals and Combination Bands

P. D. Carnegie,<sup>†</sup> A. B. McCoy,<sup>\*,‡</sup> and M. A. Duncan<sup>\*,†</sup>

Department of Chemistry, University of Georgia, Athens, Georgia 30602-2556, and Department of Chemistry, The Ohio State University, Columbus, Ohio 43210

Received: February 10, 2009; Revised Manuscript Received: March 26, 2009

Copper–water ion–molecule complexes with attached argon atoms,  $\text{Cu}^+(\text{H}_2\text{O})\text{Ar}_2$ , are produced in a supersonic molecular beam by pulsed laser vaporization. These systems are mass-selected in a reflectron time-of-flight spectrometer and studied with infrared photodissociation spectroscopy. The vibrational spectra for these complexes are characteristic of many cation–water systems, exhibiting symmetric and asymmetric O–H stretch fundamentals, and weaker features at higher frequency that have been tentatively assigned to combination bands. Using isotopically substituted spectra and model potential calculations, we are able to assign the combination bands to a water torsional vibration (frustrated rotation) in combination with the asymmetric stretch fundamental. This combination band assignment is likely to apply to IR spectra of many cation–water complexes.

### 1. Introduction

Transition metal ion solvation is a central focus of aqueous chemistry, involving covalent, electrostatic, and hydrogen bonding.<sup>1,2</sup> Gas phase clusters have provided experimental probes of the fundamental interactions involved in solvation,<sup>3–20</sup> and computational chemistry has examined these same finite sized systems with ever-increasing proficiency.<sup>21–30</sup> Mass spectrometry measurements have provided cation–solvent bonding energetics,<sup>3,4</sup> but structural information necessarily comes from spectroscopy. Although there have been electronic<sup>5–8</sup> and photoelectron spectroscopy measurements,<sup>9,10</sup> the greatest new insights have come from infrared spectroscopy on mass-selected cation–water complexes, particularly in the O–H stretching region.<sup>11–20</sup> Even for monohydrated ion complexes, however, unanticipated vibrational structure (more bands than expected) often occurs in the O–H stretching region of these spectra. We investigate this issue here in detail with a combined experimental and theoretical study of  $\text{Cu}^+(\text{H}_2\text{O})$  and  $\text{Cu}^+(\text{D}_2\text{O})$  complexes.

Infrared spectroscopy of cation–water complexes usually employs the method of mass-selected photodissociation spectroscopy.<sup>11–20</sup> Because the density of ions is so low, normal absorption methods are precluded. Photodissociation spectroscopy measures either the depletion of the selected ion or the yield of a specific fragment as a function of the infrared frequency. However, an additional caveat to these measurements is that cation–water binding energies are usually greater than infrared photon energies. For example, the symmetric and asymmetric O–H stretches of water in these complexes are expected near  $3700\text{ cm}^{-1}$  ( $10.6\text{ kcal/mol}$ ),<sup>31</sup> whereas  $\text{M}^+(\text{H}_2\text{O})$

binding energies are typically  $25\text{--}40\text{ kcal/mol}$  ( $8700\text{--}14\,000\text{ cm}^{-1}$ ).<sup>3,4</sup> To overcome this difficulty, photodissociation experiments typically employ a rare gas “tag” or “spectator” atom (Ar or Ne), whose binding energy is much lower so that it can be eliminated efficiently with vibrational excitation. The tagging method has been employed by our group<sup>13–17,19</sup> and those of Lisy<sup>11,12</sup> and Ohashi<sup>18</sup> to study the infrared spectroscopy of a variety of metal cation–water complexes. These studies find that metal ion binding causes the O–H stretches of water to be shifted to the red by  $20\text{--}80\text{ cm}^{-1}$  from the frequencies of the isolated water molecule. The presence of the cation bound to water also enhances the IR intensities of the O–H stretching vibrations compared to those in water itself, with the symmetric stretch gaining a disproportionate intensity. In rotationally resolved studies, possible for only certain complexes, the H–O–H bond angle in the water molecule is found to expand upon binding to a cation.<sup>13,14,19</sup>

Although the rare gas tag atoms used for IR photodissociation spectroscopy are essential to the experiment, their presence may also introduce small shifts in the spectra. These effects have been well documented and are usually accounted for using computational studies of the bare cation–water complex compared to the corresponding argon-tagged system.<sup>13–17,19</sup> In complexes with one or two water molecules, the tag atom usually attaches directly to the metal cation, inducing shifts in vibrational bands of only a few  $\text{cm}^{-1}$ . Much larger shifts (usually to the red) are found when the rare gas binds on the OH group of water.<sup>15</sup> If the tag atom attaches on the  $C_2$  symmetry axis of a monowater complex, K-type rotational structure may be resolved even with the typical  $1\text{ cm}^{-1}$  resolution of these experiments.<sup>14,19</sup> If the rare gas attaches off the symmetry axis, or if there is a second water molecule present, the rotational constant is much smaller and the widely spaced structure is not present. The surprising and heretofore unexplained observation in these spectra is that there are often

\* Corresponding authors. M.A.D.: e-mail, maduncan@uga.edu; fax, 706-542-1234. A.B.M.: e-mail, mccoy@chemistry.ohio-state.edu; fax, 614-292-1685.

<sup>†</sup> University of Georgia.

<sup>‡</sup> The Ohio State University.

additional vibrational bands appearing higher in frequency from and smaller in intensity than the fundamental transitions. Because the rare gas is present, these new features have often been assumed to arise from *combination bands* in which one of its vibrations adds to one of the O–H stretch fundamentals. However, no specific assignment has yet been made for these higher frequency bands.

In the present study, we investigate the infrared spectroscopy of  $\text{Cu}^+$ –water complexes tagged with argon. Copper complexes are representative of other transition metal–water systems and have been studied previously with ion chemistry,<sup>3,4</sup> spectroscopy,<sup>9,10,18,20</sup> and theory.<sup>18,21–30</sup> Infrared measurements have been reported for the singly<sup>18</sup> and doubly<sup>20</sup> charged copper cation–water complexes. In a systematic study here of the  $\text{Cu}^+(\text{H}_2\text{O})$  and  $\text{Cu}^+(\text{D}_2\text{O})$  species, IR spectroscopy and computational methods investigate the fundamental vibrations in the O–H stretching region and the additional unassigned vibrational bands in this same region. The assignments derived here provide general insight into the patterns seen for many other cation–water complexes.

## 2. Experimental Methods

$\text{Cu}^+(\text{H}_2\text{O})$ ,  $\text{Cu}^+(\text{D}_2\text{O})$ , and their complexes with argon are produced in a molecular beam by laser vaporization in a pulsed-nozzle source. The ionized complexes are cooled via a supersonic expansion, detected and size-selected with a reflectron time-of-flight (RTOF) mass spectrometer, and studied with infrared photodissociation spectroscopy in the O–H and O–D stretching region. The operation of the molecular beam instrument and mass spectrometer for these experiments has been described previously.<sup>6,13</sup> Ionized complexes are extracted from the molecular beam via pulsed acceleration fields and size-selected via their flight time through an initial flight tube section of the RTOF instrument. IR excitation occurs in the turning region of the reflectron field, and then fragment ions are mass analyzed by their flight time through a second drift tube section. The ion signals from the RTOF are collected with an electron multiplier tube detector and transmitted to a digital oscilloscope (LeCroy). The oscilloscope output is transferred to a PC computer via an IEEE-488 interface, where the fragment ion intensity from a selected parent ion is recorded as a function of the infrared laser wavelength. The infrared laser used for these experiments is an optical parametric oscillator/amplifier (OPO/OPA) system (LaserVision) employing KTA and KTP crystals pumped by a Nd:YAG laser (Continuum 8010). In the O–H (O–D) stretching region of this experiment, this laser provides several mJ/pulse of tunable IR radiation with a line width of about  $1.0\text{ cm}^{-1}$ .

## 3. Theoretical Methods

To investigate the vibrational structure in the region of the OH stretch fundamentals in the  $\text{Cu}^+(\text{H}_2\text{O})\text{Ar}_2$  complex, we identified several stationary points on the potential surface at the MP2/6-311+G(d,p) level of theory/basis set and evaluated potential and dipole surfaces as functions of the two OH bond lengths and the rotation of the water molecule about its symmetry axis, with all other internal coordinates set equal to their values at the potential minimum. This potential energy surface includes the minimum on the global surface in which the six atoms are nearly planar. It also comes close to the first-order saddle point in the  $C_s$  structure in which the water molecule has been rotated  $90^\circ$  about its symmetry axis. To assess the accuracy of this surface, we also evaluated the electronic energies and harmonic frequencies at these two stationary points

at the MP2/6-311+G(d,p) level of theory/basis. Based on these calculations, the barrier for rotation of water is  $98\text{ cm}^{-1}$ . All of the calculations were performed using the Gaussian 03 program package.<sup>32</sup> The full details of the computed structures for the  $\text{Cu}^+(\text{H}_2\text{O})\text{Ar}_{0,1,2}$  complexes are given in the Supporting Information.

The three-dimensional potential and dipole surfaces were evaluated by fitting electronic energies over a range of OH bond lengths from 0.664 to 1.264 Å and over the full range of angles. These were fit to a product of a polynomial expansion in the OH bond displacements and an expansion in  $\sin(n\tau)$  and  $\cos(n\tau)$  for the water rotation. The coefficients for the fit surfaces are provided in the Supporting Information. Because the potential coupling between the stretch and bend coordinates is small, the calculation of the vibrational energies and wave functions was performed in two steps. The ten lowest energy eigenvalues of the two-dimensional stretch Hamiltonian,

$$\hat{H}_{2d} = -\frac{\hbar^2}{2} \left( \frac{1}{m_H} + \frac{1}{m_O} - \frac{2 \cos \theta_{\text{HOH}}}{m_O} \right) \frac{\partial^2}{\partial a^2} - \frac{\hbar^2}{2} \left( \frac{1}{m_H} + \frac{1}{m_O} + \frac{2 \cos \theta_{\text{HOH}}}{m_O} \right) \frac{\partial^2}{\partial s^2} + V_{2d}(a,s) \quad (1)$$

were obtained in a direct product basis with twenty harmonic oscillator functions in the symmetric and asymmetric stretch. For this calculation, the HOH angle is equal to its calculated equilibrium value of  $107.081^\circ$ . The 10 lowest energy eigenstates of  $\hat{H}_{2d}$  were combined with the 51 Fourier functions of  $\tau$  to generate the final basis set, within which the full Hamiltonian,

$$\hat{H}_{3d} = \hat{H}_{2d} + \frac{1}{2I_{\text{BB}}(a,s)} \hat{j}^2 + [V(a,s,\tau) - V_{2d}(a,s)] \quad (2)$$

was evaluated and solved. Here  $I_{\text{BB}}$  is the moment of inertia of the water molecule with respect to its symmetry axis, which has been set at the bisector of the HOH angle.

## 4. Results and Discussion

It is not possible to study  $\text{Cu}^+(\text{H}_2\text{O})$  complexes with single photon infrared photodissociation in the O–H stretching region. The cation–water bond energy ( $38.4\text{ kcal/mol}$ ;  $13\,430\text{ cm}^{-1}$ )<sup>4</sup> is too large for photodissociation at the IR energies ( $3500\text{--}3800\text{ cm}^{-1}$ ) of these vibrations. Therefore, we employ the method of rare gas tagging with argon. We find experimentally that IR excitation also cannot eliminate argon from the singly tagged  $\text{Cu}^+(\text{H}_2\text{O})\text{Ar}$  complex, presumably because the binding energy of argon in this system also exceeds the IR photon energy in the OH stretching region. This is reasonable, because the  $\text{Cu}^+$ –Ar diatomic bond energy is calculated to be  $9\text{--}11.5\text{ kcal/mol}$  ( $3200\text{--}4000\text{ cm}^{-1}$ ) depending on the level of theory.<sup>33</sup> Ohashi and co-workers were able to photodissociate  $\text{Cu}^+(\text{H}_2\text{O})\text{Ar}$  previously,<sup>18</sup> but the spectra obtained were broad and nearly structureless, consistent with multiphoton processes or the preferential dissociation of complexes that had significant internal energy. Because our complexes are colder, and the singly charged species do not dissociate, we make the doubly tagged complexes,  $\text{Cu}^+(\text{H}_2\text{O})\text{Ar}_2$ . These species do fragment efficiently via IR excitation in the OH stretching region. We have found in other studies that such double tagging is often necessary to obtain photodissociation of transition metal cation–water complexes because of the high  $\text{TM}^+$ –Ar binding energies.<sup>16,19,34</sup> Figure 1 shows the resulting infrared photodissociation spectra for the  $\text{Cu}^+(\text{H}_2\text{O})\text{Ar}_2$  and  $\text{Cu}^+(\text{D}_2\text{O})\text{Ar}_2$  complexes measured in the mass channel corresponding to the loss of one argon atom.

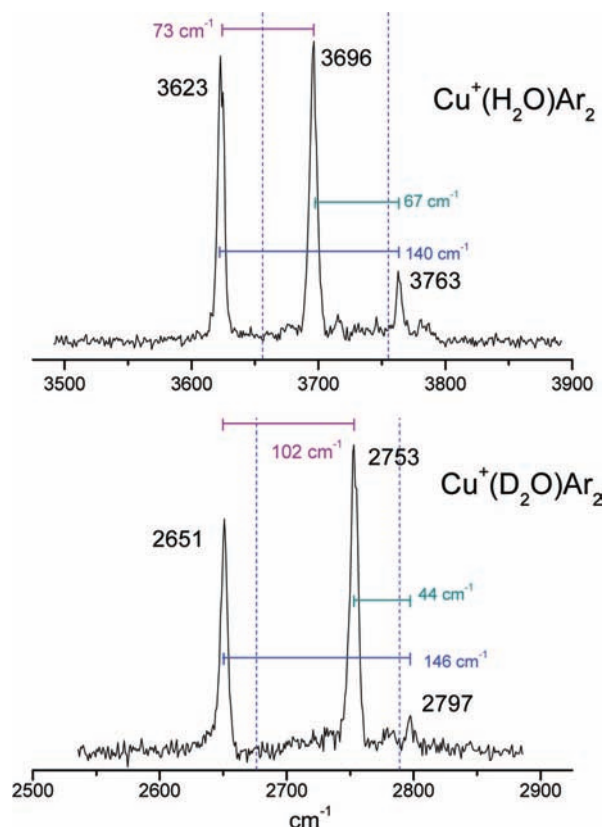


**Figure 1.** IR photodissociation spectra of  $\text{Cu}^+(\text{H}_2\text{O})\text{Ar}_2$  and  $\text{Cu}^+(\text{D}_2\text{O})\text{Ar}_2$ .

The spectra for both of these complexes contain two main features with comparable intensities that occur near the respective O–H and O–D stretches in the isolated  $\text{H}_2\text{O}$  and  $\text{D}_2\text{O}$  molecules. We therefore assign these to the expected IR-active symmetric and asymmetric stretches for these cation–water systems. The main bands for  $\text{Cu}^+(\text{H}_2\text{O})\text{Ar}_2$  occur at 3623 and 3696  $\text{cm}^{-1}$ , which are 34 and 60  $\text{cm}^{-1}$ , respectively, to the red from the corresponding bands in  $\text{H}_2\text{O}$ .<sup>31</sup> Likewise, the  $\text{Cu}^+(\text{D}_2\text{O})\text{Ar}_2$  complex has bands at 2651 and 2753, which are red-shifted by 20 and 35  $\text{cm}^{-1}$  from the corresponding bands in  $\text{D}_2\text{O}$ .<sup>31</sup> These red-shifted vibrations are similar to those that have now been observed and discussed for many metal ion–water complexes.<sup>11–20,34</sup> The cation in these complexes binds to the water closest to the oxygen atom in a  $C_{2v}$  configuration, consistent with the prediction for a charge–dipole interaction. However, in addition to the expected electrostatic interaction, transition metal ions also bind to water via partial covalent forces. The overall interaction leads to charge transfer from the water orbitals containing the lone pair electrons, and these orbitals have bonding character along the O–H bonds. The polarization of these orbitals toward the metal ion reduces the effective bonding in the water moiety, leading to a reduction in the O–H force constant and the red-shifted vibrational frequencies. The trend of this effect for the first row transition metal ions has been studied recently by our group.<sup>34</sup> The band positions and red shifts seen here for  $\text{Cu}^+$  are very close to those measured for other late transition metal ion complexes ( $\text{Ni}^+$ ,  $\text{Co}^+$ ) with water.<sup>16,34</sup>

Another interesting aspect of the vibrational spectra for these copper–water complexes is the ratio of the intensities of the symmetric and asymmetric stretching bands. In the free water molecule, the asymmetric stretch is about 18 times more intense than the symmetric stretch.<sup>35</sup> However, in the present spectra,

these bands are comparable in intensity. Again, this effect has been documented and discussed for several other metal cation–water complexes.<sup>11–20,34</sup> The intensity of IR bands depends on the dipole derivative of the vibrating system, and this is strongly enhanced when vibration takes place next to an ion. As demonstrated by the combined studies of theory and experiment, both the symmetric and asymmetric stretch vibrations gain intensity in cation complexes compared to the isolated water molecule. However, the symmetric stretch modulates the dipole more effectively than the asymmetric stretch, gaining more IR intensity, and therefore these two bands have comparable intensities in the spectrum. Again, the intensity ratios of the bands here are much the same as those seen for  $\text{Ni}^+$  and  $\text{Co}^+$  complexes with water.<sup>16,34</sup>

Both the spectrum of  $\text{Cu}^+(\text{H}_2\text{O})\text{Ar}_2$  and that of  $\text{Cu}^+(\text{D}_2\text{O})\text{Ar}_2$  have additional weak vibrational bands higher in frequency than the main two intense bands. These appear at 3763  $\text{cm}^{-1}$  for the  $\text{H}_2\text{O}$  complex and 2797  $\text{cm}^{-1}$  for the  $\text{D}_2\text{O}$  species. Weaker vibrational bands like these have now been seen in the infrared spectra for many cation–water complexes when these systems are studied with rare gas tagging.<sup>11–20,34</sup> Because of their position at higher energy and because these bands are not detected unless a rare gas atom is present, they have generally been attributed to some sort of combination band involving a rare gas stretching vibration and one or the other of the O–H stretching vibrations. However, a detailed explanation of these combination bands has not been provided. To investigate this issue further, we have measured the spectrum for the  $\text{D}_2\text{O}$  system, as shown here, to try to identify these bands by their isotopic shifts. We also have investigated these systems with computational studies to identify the vibrations via their frequencies and isotopic shifts.

The deuteration experiment immediately provides insight into the likely nature of the high frequency band. In the  $\text{Cu}^+(\text{H}_2\text{O})\text{Ar}_2$  spectrum, this band appears at 3763  $\text{cm}^{-1}$ . As shown in Figure 1, this position is 67  $\text{cm}^{-1}$  to the blue from the asymmetric stretch band and 140  $\text{cm}^{-1}$  to the blue from the symmetric stretch band. Initially, then, it is not clear which of the OH fundamentals the combination is built on, and what the frequency is for the other vibration. However, deuteration leads to a high frequency band at 2797  $\text{cm}^{-1}$ . This is 44  $\text{cm}^{-1}$  to the blue from the asymmetric stretch and 146  $\text{cm}^{-1}$  to the blue from the symmetric stretch. The interval above the symmetric stretch has therefore increased upon deuteration, suggesting that this cannot be where the combination occurs. On the other hand, the interval above the asymmetric stretch decreased from 67 to 44  $\text{cm}^{-1}$ , completely within the range of reasonable isotopic shifts. Therefore, the combination involves the asymmetric stretch and the frequency of the mode in combination with this is about 67  $\text{cm}^{-1}$  for  $\text{Cu}^+(\text{H}_2\text{O})\text{Ar}_2$ .

To explore these issues further, we have computed the minimum energy structure for the  $\text{Cu}^+(\text{H}_2\text{O})\text{Ar}_2$  complex, which is depicted in Figure 2. In this structure, the six atoms are coplanar with one argon atom forming an 163.5° Ar–Cu–O angle and the second forming an Ar–Cu–O angle of 100.8°. The unscaled vibrational frequencies are presented in Table 1 for both the  $\text{H}_2\text{O}$  and  $\text{D}_2\text{O}$  complexes. If we apply the recommended scaling factor (0.9496) to these vibrations,<sup>36</sup> we obtain symmetric and asymmetric stretches of 3638 and 3732  $\text{cm}^{-1}$  for the  $\text{H}_2\text{O}$  species and 2623 and 2737  $\text{cm}^{-1}$  for the  $\text{D}_2\text{O}$  species, in good agreement with the experimental band positions. Comparison of these values to the computed frequencies for  $\text{Cu}^+(\text{H}_2\text{O})$  and  $\text{Cu}^+(\text{H}_2\text{O})\text{Ar}$  (see Supporting Information) shows that argon induces only a small shift on the vibrations of the untagged complex ( $<10 \text{ cm}^{-1}$ ). Five frequencies are computed



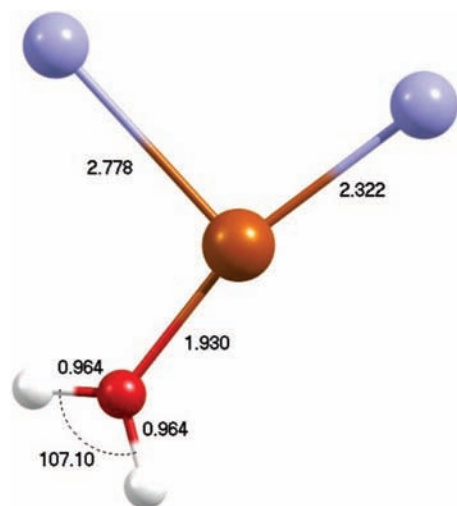


**Figure 2.** Minimum energy structure of  $\text{Cu}^+(\text{H}_2\text{O})\text{Ar}_2$ .

**TABLE 1: Computed Vibrations (Unscaled) and Intensities of  $\text{Cu}^+(\text{H}_2\text{O})\text{Ar}_2$  and  $\text{Cu}^+(\text{D}_2\text{O})\text{Ar}_2$  Complexes<sup>a</sup>**

| $\text{Cu}^+(\text{H}_2\text{O})\text{Ar}_2$ | $\text{Cu}^+(\text{D}_2\text{O})\text{Ar}_2$ | assignment            |
|--|--|-----------------------|
| 30.8 (1.45)                                  | 29.6 (1.28)                                  | Ar–Cu–HOH ip bend     |
| 46.9 (1.21)                                  | 46.2 (4.94)                                  | Ar–Cu–HOH bend        |
| 64.2 (50.8)                                  | 47.4 (32.8)                                  | H–O–H oop rotation    |
| 68.0 (29.7)                                  | 65.1 (0.22)                                  | mixed Ar motion       |
| 79.5 (9.63)                                  | 78.2 (8.78)                                  | Cu–Ar stretch         |
| 133.9 (212.2)                                | 99.5 (117.4)                                 | HOH oop bend          |
| 174.1 (6.71)                                 | 172.7 (6.28)                                 | Cu–Ar stretch         |
| 408.5 (7.53)                                 | 391.9 (7.35)                                 | Cu–HOH stretch        |
| 608.9 (84.0)                                 | 455.0 (41.1)                                 | HOH ip bend           |
| 1669.1 (94.8)                                | 1226.9 (51.1)                                | HOH scissors bend     |
| 3831.5 (139.0)                               | 2762.6 (81.2)                                | OH symmetric stretch  |
| 3929.5 (245.8)                               | 2882.7 (134.8)                               | OH asymmetric stretch |

<sup>a</sup> Frequencies are in  $\text{cm}^{-1}$ , and intensities (in parentheses) are in  $\text{km/mol}$ .

for  $\text{Cu}^+(\text{H}_2\text{O})\text{Ar}_2$  with frequencies below  $100 \text{ cm}^{-1}$ . Of these, the Cu–Ar stretch is predicted to have a frequency near  $80 \text{ cm}^{-1}$ , but this is not predicted to change substantially upon deuteration. Another vibration involving mixed argon motion occurs at  $68 \text{ cm}^{-1}$ , but again, little isotopic shift is predicted. However, the H–O–H out-of-plane torsional motion is predicted to have a frequency (unscaled) of about  $68 \text{ cm}^{-1}$ , which is reduced to about  $48 \text{ cm}^{-1}$  upon deuteration. This latter behavior is consistent with the magnitude of the interval and the isotopic shift seen for our combination band.

To investigate this assignment for the combination band in more detail, we developed a three-dimensional potential and dipole moment surfaces as functions of the two OH distances and the rotation of the water molecule about its symmetry axis. In the absence of the argon atoms, the torsional motion would correlate to rotation of  $\text{Cu}^+(\text{H}_2\text{O})$  about its symmetry axis. The results of these calculations for  $\text{Cu}^+(\text{H}_2\text{O})\text{Ar}_2$  are plotted in Figure 3. Here we show the potential as a function of the rotation of the water molecule,  $\tau$ , with the thick black curve. The three one-dimensional surfaces are obtained by averaging the three-dimensional potential over the specified stretch vibration. Superimposed on this curve are projections of the probability amplitudes onto  $\tau$ , plotted at their calculated energy.

As the fit potential has a barrier to water rotation of  $109.2 \text{ cm}^{-1}$ , the ground state wave function has a splitting of  $1.6 \text{ cm}^{-1}$  for  $\text{Cu}^+(\text{H}_2\text{O})\text{Ar}_2$  and  $0.14 \text{ cm}^{-1}$  in  $\text{Cu}^+(\text{D}_2\text{O})\text{Ar}_2$ . This doublet is depicted by the red and black curves. As the stretch/bend

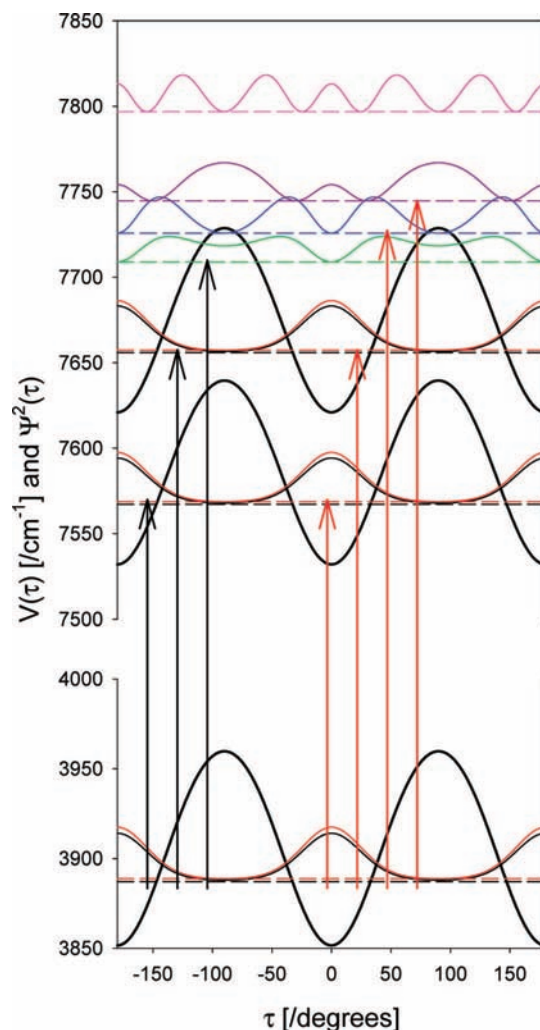


**Figure 3.** Calculated one-dimensional potential surface obtained by averaging the three-dimensional potential over the specified stretch vibrations of  $\text{Cu}^+(\text{H}_2\text{O})\text{Ar}_2$ . The thick black curves are those for the adiabatic potentials for the ground state and for excited states with one quanta in the symmetric and asymmetric stretches. The horizontal lines are the vibrational energies of each state for which there is some noticeable intensity. The red curve overlapping another black one is the ground state in the bending coordinate on each surface. The green, blue, purple, and pink curves give the probability amplitudes for the next four states on the asymmetric stretch potential. The black and red arrows show transitions originating from the two nearly degenerate states (plotted in red and black).

couplings are weak, the splittings of the levels with one quantum in either of the OH stretches are also  $1.6$  and  $0.14 \text{ cm}^{-1}$ . This splitting increases with excitation and the energy difference between next pair of states is  $18 \text{ cm}^{-1}$  in  $\text{Cu}^+(\text{H}_2\text{O})\text{Ar}_2$  and  $3 \text{ cm}^{-1}$  in  $\text{Cu}^+(\text{D}_2\text{O})\text{Ar}_2$ . The probability amplitudes for these four states, as well as the next two states in the bend progression are plotted on top of the corresponding potential energy surface in Figure 3.

Figure 4 depicts the calculated spectra for  $\text{Cu}^+(\text{H}_2\text{O})\text{Ar}_2$  and  $\text{Cu}^+(\text{D}_2\text{O})\text{Ar}_2$  compared to the experimental spectra. Here we have weighted the transitions originating from the members of the tunneling doublet in  $\text{Cu}^+(\text{H}_2\text{O})\text{Ar}_2$  in a 1:3 ratio, to account for the fact that the hydrogen atoms are fermions. In  $\text{Cu}^+(\text{D}_2\text{O})\text{Ar}_2$  the intensities are weighed by a 2:1 ratio because deuterium is a boson. In the calculated spectrum for  $\text{Cu}^+(\text{H}_2\text{O})\text{Ar}_2$ , the two large peaks correspond to the fundamentals in the symmetric (blue) and asymmetric (red) stretch. Although the calculated transitions fall systematically at higher

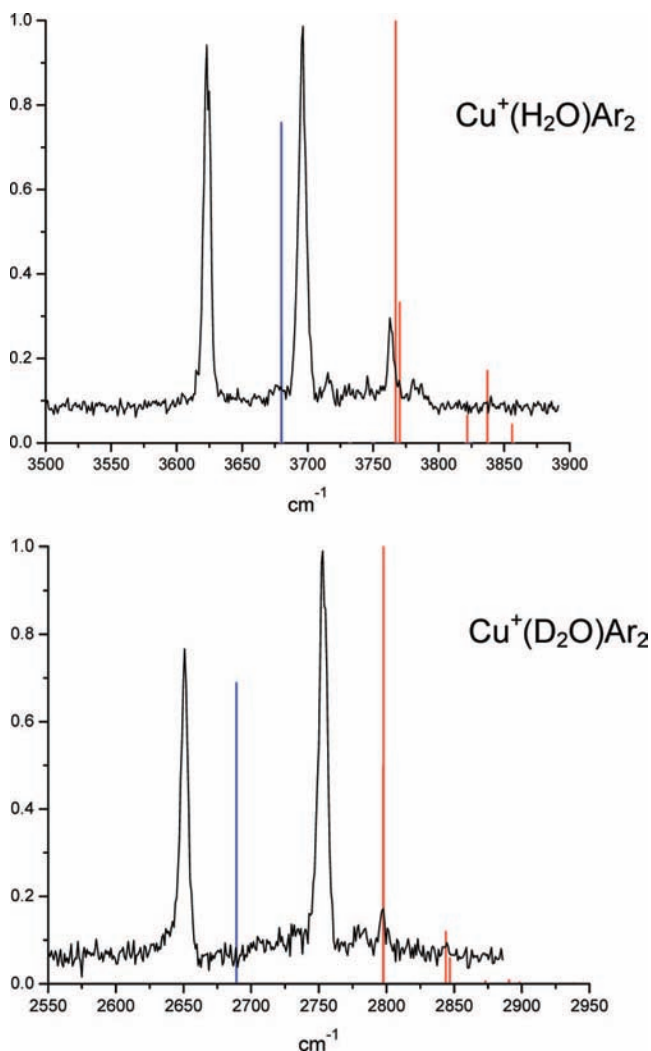


**Figure 4.** Spectra calculated for  $\text{Cu}^+(\text{H}_2\text{O})\text{Ar}_2$  (upper) and  $\text{Cu}^+(\text{D}_2\text{O})\text{Ar}_2$  (lower) using the model potentials, compared to the corresponding experimental spectra. The symmetric stretch transitions are indicated in blue, and the asymmetric stretch transitions are in red. The intensities are scaled to a relative value of 1.0 for the most intense lines in each spectrum. Although the calculated transitions are systematically offset to higher frequencies than the experimental spectra, the spacings and relative intensities calculated are in good agreement with those measured.

absolute frequencies than the measured bands, the spacings and relative intensities predicted are in good agreement with the experiment. The calculated splittings between the fundamental transitions is  $87\text{ cm}^{-1}$ , compared to the experimental value of  $73\text{ cm}^{-1}$ . The peaks plotted in red that are to the blue of the asymmetric stretch fundamental correspond to transitions to the states represented by the green blue and purple curves in Figure 3. Although three bands are predicted for  $\text{Cu}^+(\text{H}_2\text{O})\text{Ar}_2$ , only one combination band is detected experimentally. The calculated transition that corresponds to the observed transition is the one that terminates in the state shown in blue in Figure 3. It is not clear whether this disagreement is caused by the limited sensitivity of the experiment or by sensitivities of the computed multiplet splitting and/or line intensities to the level of electronic structure theory or to couplings to the twelve vibrational degrees of freedom that have not been considered in the present study. However, the spacing calculated from the asymmetric stretch fundamental to the most intense combination feature is  $70\text{ cm}^{-1}$  compared to the experimental value of  $67\text{ cm}^{-1}$ . The relative intensities of these combination bands compared to the funda-

mentals are comparable to those in the recorded spectrum. There is also a very small feature at  $3910\text{ cm}^{-1}$  in the calculated spectrum (not shown in the figure). It corresponds to the transition to the state shown in pink in Figure 3.

Analogous assignments can be made for the calculated spectrum of  $\text{Cu}^+(\text{D}_2\text{O})\text{Ar}_2$ . The heavier mass of deuterium leads to a decrease in the energies of the states involved and now the four lowest energy states are below the potential barrier. As a result, the calculated spectrum predicts only one pair of combination peaks with significant intensity to the blue of the asymmetric stretch fundamental. As a result, the agreement with experiment is arguably better than for  $\text{H}_2\text{O}$ . The sym/asym fundamental spacing is calculated to be  $109\text{ cm}^{-1}$  compared to the experimental value of  $102\text{ cm}^{-1}$ , and the combination bands are calculated to be  $46\text{ cm}^{-1}$  above the asymmetric stretch, compared to the experimental value of  $44\text{ cm}^{-1}$ . Together, these model calculations show that not only do the frequencies and isotopic shifts of the torsional vibration match the experiment but also the combination bands have an expected intensity roughly matching that of the experiment.

To investigate the somewhat surprisingly strong intensity in the combination band that is observed in the spectrum, we have plotted the three components of the transition moment between the ground state and the fundamental in the asymmetric OH stretch as a function of  $\tau$ . These plots are shown in the Supporting Information for this manuscript. The magnitude of the changes in the  $c$ -component of the transition moment is found to be comparable to the  $a$ - and  $b$ -components. The symmetry of the bend wave functions and the components of the dipole lead us to conclude that the  $c$ -component is responsible for the transitions to the states plotted in blue and green whereas the  $a$ - and  $b$ -components result in the transitions to the states plotted in black, red, and purple. In the case of the transition to the fundamental in the symmetric stretch, the  $c$ -component of the transition moment is nearly zero. The physics that underlies these observations can be seen if one considers the expected  $\Delta K$  selections for  $\text{Cu}^+(\text{H}_2\text{O})$  without any argon atoms. In the absence of the argon atoms, the complex has nearly  $C_{2v}$  symmetry and although only  $\Delta K = 0$  transitions would be observed for the transition to the fundamental of the symmetric stretch, the fundamental in the asymmetric stretch would have  $\Delta K = \pm 1$  transitions. It is these  $\Delta K = \pm 1$  transitions that are seen in the spectrum. The frequency is shifted due to the fact that this motion is now a hindered rotation in the complex.

Overall, the agreement between the experimental and calculated spectra is very good, but not quantitative. As noted, there is an offset in the absolute frequencies of about  $60\text{--}70\text{ cm}^{-1}$  for  $\text{Cu}^+(\text{H}_2\text{O})\text{Ar}_2$  and about  $40\text{ cm}^{-1}$  for  $\text{Cu}^+(\text{D}_2\text{O})\text{Ar}_2$ . Given the fact that only three of the twelve vibrational degrees of freedom are considered and that the potential was calculated at the MP2/6-311+G(d,p) level of theory/basis, we would not have expected more than semiquantitative agreement. The overall picture that emerges is one in which ro-vibrational transitions in bare water become manifested as torsional combination bands built off of the asymmetric stretch in the complex. In addition, the fact that the transitions are assigned to combination bands with hindered rotation of  $\text{Cu}^+(\text{H}_2\text{O})$  about its symmetry axis makes the precise frequencies sensitive to the height of the barrier. As this will be strongly system dependent, it is expected that the precise positions and intensities of these combination bands will differ from one system to another. This is completely consistent with experimental observations.<sup>11–20,34</sup>

Free internal rotational motion of water molecules has been seen previously for a variety of van der Waals complexes with

other small molecules.<sup>37–39</sup> In a recent study completed by our group, similar free rotation of water was observed for the  $\text{Cr}^{2+}(\text{H}_2\text{O})\text{Ar}_n$  complexes.<sup>19</sup> In this latter system, the structured spectrum corresponding to this internal rotation was most apparent for the  $n = 4$  complex, but some structure was also seen for the  $n = 3$  and 5 species. An investigation of the angular potential for the  $\text{Cr}^{2+}(\text{H}_2\text{O})\text{Ar}_4$  system found essentially no barrier to internal rotation because of the symmetric arrangement of the argon atoms around the metal ion. In the present system, the arrangement of the argons is less symmetric, and consequently there is a significant barrier to internal rotation. The frustrated rotation becomes a torsional vibration, and this is the source of the combination bands seen here. This general scenario apparently applies to many hydrated metal ion complexes, where a similar combination band structure has been seen. Likewise, combination bands lying at frequencies higher than the O–H stretch fundamentals have also been seen in the spectra of protonated water clusters.<sup>40–42</sup> On the basis of the similarity of the water structures in these systems, those combination bands are also likely to arise from water torsional vibrations.

**Acknowledgment.** We acknowledge generous support for this work from the U.S. Department of Energy (M.A.D., grant no. DE-FG02-96ER14658) and the National Science Foundation (A.B.M., grant no. CHE-0515627).

**Supporting Information Available:** This material is available free of charge via the Internet at <http://pubs.acs.org> and includes the parameters used in fitting the potential surface in eq 2, the structures and frequencies for the  $\text{Cu}^+(\text{H}_2\text{O})\text{Ar}_{0,1,2}$  complexes, plots of the three components of the transition moments vs  $\tau$ , and the complete citation for ref 32.

## References and Notes

- (1) Marcus, Y. *Ion Solvation*; John Wiley: Chichester, U.K., 1985.
- (2) Burgess, J. *Ions in Solution*; Horwood Publishing: Chichester, U.K., 1999.
- (3) Magnera, T. F.; David, D. E.; Stulik, D.; Orth, R. G.; Jonkman, H. T.; Michl, J. *J. Am. Chem. Soc.* **1989**, *111*, 5036.
- (4) Dalleska, N. F.; Honma, K.; Sunderlin, L. S.; Armentrout, P. B. *J. Am. Chem. Soc.* **1994**, *116*, 3519.
- (5) Lessen, D. E.; Asher, R. L.; Brucat, P. J. *J. Chem. Phys.* **1990**, *93*, 6102.
- (6) Duncan, M. A. *Annu. Rev. Phys. Chem.* **1997**, *48*, 69.
- (7) Duncan, M. A. *Int. J. Mass Spectrom.* **2000**, *200*, 545.
- (8) Abate, Y.; Kleiber, P. D. *J. Chem. Phys.* **2005**, *122*, 084305.
- (9) Misaizu, F.; Tsukamoto, K.; Sanekata, M.; Fuke, K. *Laser Chem.* **1995**, *15*, 195.

- (10) Muntean, F.; Taylor, M. S.; McCoy, A. B.; Lineberger, W. C. *J. Chem. Phys.* **2004**, *121*, 5676.
- (11) Lisy, J. M. *Int. Rev. Phys. Chem.* **1997**, *16*, 267.
- (12) Patwari, G. N.; Lisy, J. M. *J. Chem. Phys.* **2003**, *118*, 8555.
- (13) Duncan, M. A. *Int. Rev. Phys. Chem.* **2003**, *22*, 407.
- (14) Walker, N. R.; Walters, R. S.; Pillai, E. D.; Duncan, M. A. *J. Chem. Phys.* **2003**, *119*, 10471.
- (15) Walters, R. S.; Duncan, M. A. *Aust. J. Chem.* **2004**, *57*, 1145.
- (16) Walters, R. S.; Pillai, E. D.; Duncan, M. A. *J. Am. Chem. Soc.* **2005**, *127*, 16599.
- (17) Walker, N. R.; Walters, R. S.; Duncan, M. A. *New J. Chem.* **2005**, *29*, 1495.
- (18) (a) Iino, T.; Ohashi, K.; Mune, Y.; Inokuchi, Y.; Judai, K.; Nishi, N.; Sekiya, H. *Chem. Phys. Lett.* **2006**, *427*, 24. (b) Iino, T.; Ohashi, K.; Inoue, K.; Judai, K.; Nishi, N.; Sekiya, H. *J. Chem. Phys.* **2007**, *126*, 194302.
- (19) Carnegie, P. D.; Bandyopadhyay, B.; Duncan, M. A. *J. Phys. Chem. A* **2008**, *112*, 6237.
- (20) O'Brien, J. T.; Williams, E. R. *J. Phys. Chem. A* **2008**, *112*, 5893.
- (21) Rosi, M.; Bauschlicher, C. W. *J. Chem. Phys.* **1989**, *90*, 7264.
- (22) Rosi, M.; Bauschlicher, C. W. *J. Chem. Phys.* **1990**, *92*, 1876.
- (23) Bauschlicher, C. W.; Langhoff, S. R.; Partridge, H. *J. Chem. Phys.* **1991**, *94*, 2068.
- (24) Adamo, C.; Lelj, F. *J. Mol. Struct. (THEOCHEM)* **1997**, *389*, 83.
- (25) Trachtman, M.; Markham, G. D.; Glusker, J. P.; George, P.; Bock, C. W. *Inorg. Chem.* **1998**, *37*, 4421.
- (26) Feller, D.; Glendening, E. D.; de Jong, W. A. *J. Chem. Phys.* **1999**, *110*, 1475.
- (27) El-Nahas, A. M.; Tajima, N.; Hirao, K. *THEOCHEM* **1999**, *469*, 201.
- (28) Irigoras, A.; Elizalde, O.; Silanes, I.; Fowler, J. E.; Ugalde, J. M. *J. Am. Chem. Soc.* **2000**, *122*, 114.
- (29) Taylor, M. S.; Muntean, F.; Lineberger, W. C.; McCoy, A. B. *J. Chem. Phys.* **2004**, *121*, 5688.
- (30) Gourlaouen, C.; Piquemal, J.-P.; Saue, T.; Parisel, O. *J. Comput. Chem.* **2005**, *27*, 142.
- (31) Shimanouchi, T. In *NIST Chemistry WebBook*; Linstrom, P. J., Mallard, W. G., Eds.; NIST Standard Reference Database Number 69; National Institute of Standards and Technology: Gaithersburg, MD, 2008 (<http://webbook.nist.gov>).
- (32) Frisch, M. J.; et al. *Gaussian 03*, revision B.02; Gaussian, Inc.: Pittsburgh, PA, 2003.
- (33) Shen, Y.; Belbruno, J. J. *J. Phys. Chem. A* **2005**, *109*, 10077.
- (34) Carnegie, P. D.; Bandyopadhyay, B.; Duncan, M. A. To be published.
- (35) Galabov, B.; Yamaguchi, Y.; Remington, R. B.; Schaefer, H. F. *J. Phys. Chem. A* **2002**, *106*, 819.
- (36) Scott, A. P.; Radom, L. *J. Phys. Chem.* **1996**, *100*, 16502.
- (37) Gotch, A. J.; Zwier, T. S. *J. Chem. Phys.* **1992**, *96*, 3388.
- (38) Susuki, S.; Green, P. G.; Bumgarner, R. E.; Dasgupta, S.; Goddard, W. A.; Blake, G. A. *Science* **1992**, *257*, 942.
- (39) Berden, G.; Meerts, W. L.; Schmitt, M.; Kleinermaans, K. *J. Chem. Phys.* **1996**, *104*, 972.
- (40) Yeh, L. I.; Okumura, M.; Myers, J. D.; Price, J. M.; Lee, Y. T. *J. Chem. Phys.* **1989**, *91*, 7319.
- (41) Jiang, J.-C.; Wang, Y.-S.; Chang, H.-C.; Lin, S. H.; Lee, Y. T.; Niedner-Schatteburg, G.; Chang, H.-C. *J. Am. Chem. Soc.* **2000**, *122*, 1398.
- (42) Headrick, J. M.; Diken, E. G.; Walters, R. S.; Hammer, N. I.; Christie, R. A.; Cui, J.; Myshakin, E. M.; Duncan, M. A.; Johnson, M. A.; Jordan, K. D. *Science* **2005**, *308*, 1765.

JP901231Q